THE TORSIONAL SPECTRUM OF THE HYDROGEN TRIOXIDE MOLECULE

G.A.Pitsevich[a*], A.E.Malevich[a], U.U.Sapeshka[b]

[a] Faculty of Physics, Belarusian State University, ,Minsk, Belarus.
[b] University of Illinois, Chicago, USA
*Corresponding author. E-mail address: pitsevich@bsu.by (George Pitsevich).

KEYWORDS: torsional vibrations, potential barriers, hydrogen trioxide, potential energy surface, DVR, internal rotation, conformers, non-rigid molecules, Fourier analysis

Abstract

The energies of the stationary torsional levels of the hydrogen trioxide molecule were calculated at the B3LYP, MP2, and CCSD(T) levels of theory using augmented correlation consistent acc-pVTZ basis set. The molecular symmetry group whose elements are inherent to both equilibrium conformer's symmetry elements (C_2 and C_S) of the HT molecule was found. Different methods of the molecular parameters calculations were suggested and analyzed. The torsional, spin and total wave functions were classified by irreducible representations of the $C_{2V}(M)$ molecular symmetry group. The 2D dipole moment surface was calculated too. The energies of the stationary torsional states were found using DVR and Fourier methods. With this and acceptable combinations of spatial and spin wave functions, the IR torsional spectrum was calculated at different temperatures. The tunneling frequencies in the ground and some excited torsional states were estimated too.

1. INTRODUCTION

The hydrogen trioxide (HT) molecule HOOOH in many ways is a benchmark object. Firstly, this molecule is the second after hydrogen hydroxide representative of the series of hydrogen polyoxides specified by the formula HO_nH (n=1,2,3,4,5….), the researchers' interest to which is undoubtedly increasing in recent times [1-4]. Secondly, the HT molecule is the simplest representative of a whole series of molecules having two equivalent non-coaxial internal tops. Thirdly, the molecule is capable of forming the cluster structures due to the formation of hydrogen bonds. Besides, the HT molecule has two equilibrium configurations, which differ in the mutual orientation of hydroxyl groups. Finally, the HT is potentially non-rigid molecule since each of the two conformers can exist in two configuration equivalent versions, even though, the matter of the real rigidity or non-rigidity has yet to be analyzed. Many researchers also point out the significant role of the HT molecule in oxidizing processes that are taking place in atmospheric phenomena [3,5,6] and biological systems [3,7,8], as well as in other significant chemical reactions [9-15]. In addition, hydrogen and oxygen atoms are included in a set of 11

elements of the "astronomical periodic table of elements" [16]. Consequently, an HT molecule can be of interest in astronomical applications.

The low stability of the molecule being studied makes the performance of the spectral investigations considerably more difficult. The first success in registering the IR and Raman spectra of the HT molecule belongs to a group of scientists under the leadership of Giguère in the early 1970s [17-19]. However, the presence of a number of other polyoxides in the samples made it possible to make only some preliminary assignments in the experimental spectra. The detailed interpretation of the IR spectrum of HT registered in argon matrix was proposed by Engdahl and Nelander in 2002 [20], and in 2005, Suma registered a purely rotational spectrum of the HT molecule [21].

The theoretical investigations of the potential energy surface (PES) and spectra of the HT molecule were started simultaneously with the beginning of the spectral investigations [22-24]. In 1978, Cremer examined in detail how the basic set choice and the way of accounting of the electron correlation affects the structural and energetic parameters of the molecule [25]. On the PES, the global and local minima, transition states were revealed as well as the characteristics of HT were compared with those of hydroxide peroxide [26]. The investigations of the PES were continued in the papers [27-29], while the mechanisms [30] and enthalpies [31,32] of the formation of the HT molecule and methods of its synthesis [33,34] were determined by quantum-chemical methods in a number of papers.

As we know, the calculation of the normal vibrations of the HT molecule was firstly performed in paper [19]. Later the calculations of the IR spectra of the molecule using the quantum-chemical methods were continued in the papers [29,35,36]. In the first of these papers, the structures and IR spectra were calculated using the CASSCF method and augmented by diffuse and second sets of polarization functions basis set. In the paper [36], the respective calculations were performed on the CCSD(T)/cc-pVXT (X=T,Q,5,6) levels of the theory although the anharmonic calculations of the IR spectrum were performed using the DFT methods. In the paper [29], the calculations of the structure and IR spectra of the TH were performed using the explicitly correlated techniques (CCSD(T)-F12/cc-pVTZ-F12) taking into account the anharmonicity effects. Many interesting aspects concerning the structure, spectral as well as physical and chemical characteristics of the HT molecule can be extracted from recent reviews [37,38].

As follows from the review presented, the researchers' interest in the HT molecule does not wane. Many spectral and structural characteristics of the molecule are becoming more accurate as new improved methods in quantum chemistry appear. However, one of the most interesting and important aspects, which is the internal rotation of the two hydroxyl groups, has not yet been

studied. The question of whether the HT molecule is rigid or nonrigid object has yet to be answered. These problems will be the main objective of this paper. To give the answers to these questions, first of all, in section 2 we analyze the symmetry properties of the molecule. Then in Section 3, we will discuss the mathematical backgrounds of calculations and different methods of data preparation. In Section 4 we compare the results obtained using DVR and Fourier methods for the numerical solution of the Schrödinger equation. In Section 5 we discuss the results of torsional levels energy calculations and simulate the torsional IR spectra of both conformers of the HT molecule. In Section 6 some conclusions will drow.

2. MOLECULAR SYMMETRY GROUP

The rigidity or nonrigidity of the HT molecule is determined by its capability of tunneling from one configuration to another, which depends on the height and shape of the potential barrier separating equivalent configurations. If there is no tunneling, the order of a group of the molecular symmetry [39,40] HT is equal to that of its point symmetry group (C_2) [41]. If the tunneling takes place, the order of HT molecular symmetry group can be determined using the results of the paper [42], according to which the order of the molecular symmetry group is equal to the product of the order of the point symmetry group by the number of the configuration versions of the nonrigid molecule. Since the group order C_2 is equal to two and there are two HT versions, the order of the molecular symmetry group is four. One can find that the molecular symmetry group of the HT molecule contains four symmetry elements: E, (12)(34), E^*, $(12)(34)^*$ and, in accordance with [40], this molecular symmetry group may be called $C_{2V}(M)$. Note that all these symmetry elements are inherent to both equilibrium conformers symmetry elements (C_2 on the left in Fig.1 and C_S in the middle in Fig.1) of the HT molecule.

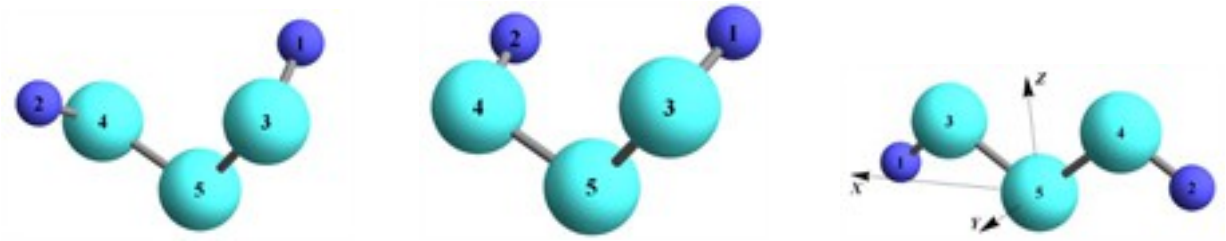

Figure 1. The equilibrium configuration of the trans- (on the left) and cis- (in the middle) conformers of TH molecule as well as the flat configuration with C_{2V} symmetry being the initial one for performing the calculations of the 2D PES where both torsional coordinates are zero (on the right).

Table 1 represents the irreducible representations of the $C_{2V}(M)$ molecular symmetry group for the HT molecule.

Table 1 The table of irreducible representations of the $C_{2V}(M)$ molecular symmetry group adapted for the HT molecule [40]. Atomic numbering is the same as in Fig.1

$C_{2V}(M)$	E	(12)(34)	E^*	$(12)(34)^*$
Short name	P_1	P_2	P_3	P_4
A_1	1	1	1	1
A_2	1	1	-1	-1
B_1	1	-1	1	-1
B_2	1	-1	-1	1

The symmetry properties of the 2D surfaces of the potential energy, dipole momentum and kinematic coefficients of the HT molecule are very close to those of the methanediol molecule (MD), for which the internal rotation was recently analyzed [43]. In [43] the symmetry elements of the 2D surfaces were connected with symmetry elements of the $C_{2V}(M)$ molecular symmetry group. According to [43] let's call the plane which is perpendicular to the coordinate plane γ,φ and intersect it along diagonal (0^0,0^0 – 360^0,360^0) plane 1. The plane which is perpendicular to the coordinate plane γ,φ and intersects it along diagonal (0^0,360^0 – 360^0,0^0) will be plane 2. The intersection of these two planes will be the C_2 symmetry axis. Then these elements will be connected with symmetry elements of the $C_{2V}(M)$ group according to data from Table 2. In addition, the transformations of the torsional coordinates γ,φ under the action of the $C_{2V}(M)$ symmetry operations include in Table 2 too.

Table 2. The transformations of the torsional coordinates under the action of the $C_{2V}(M)$ symmetry operations and interconnection of the symmetry elements of the 2D surfaces of the PES, wave functions with the $C_{2V}(M)$ symmetry operations of the HT molecule.

$C_{2V}(M)$	E	(12)(34)	E^*	$(12)(34)^*$
Short name	P_1	P_2	P_3	P_4
Symmetry elements of the 2D surfaces	E	Reflection in plane 1	Rotation around C_2 axis	Reflection in plane 2
Transformations of the torsional coordinates	γ,φ	φ,γ	$-\gamma,-\varphi$	$-\varphi,-\gamma$

Using Table 1 and 2 one can classify the torsional wave functions of the HT molecule by visual analysis or by the following formulas:

$$if\ \left|\Psi_k(\gamma,\varphi)-P_j\Psi_k(\gamma,\varphi)\right|=\left|\Psi_k(\gamma,\varphi)-\Psi_k\left(P_j(\gamma,\varphi)\right)\right|=0\ \Rightarrow \chi_{i,j}=1 \qquad (1)$$

$$if\ \left|\Psi_k(\gamma,\varphi)+P_j\Psi_k(\gamma,\varphi)\right|=\left|\Psi_k(\gamma,\varphi)+\Psi_k\left(P_j(\gamma,\varphi)\right)\right|=0\ \Rightarrow \chi_{i,j}=-1 \qquad (2)$$

The results of the transformations of some molecular characteristics under $C_{2V}(M)$ symmetry operations are collected in Table 3.

Table 3 The symmetry species and results of the transformations of some HT molecular characteristics (see (6) and (15)) under $C_{2V}(M)$ molecular symmetry group.

Molecular characterictic	Symmetry operators				Irreducible representations
	P_1	P_2	P_3	P_4	
$U(\gamma,\varphi)$	$U(\gamma,\varphi)$	$U(\varphi,\gamma)$	$U(-\gamma,-\varphi)$	$U(-\varphi,-\gamma)$	A_1
$F_{\gamma\varphi}(\gamma,\varphi)$	$F_{\gamma\varphi}(\gamma,\varphi)$	$F_{\gamma\varphi}(\varphi,\gamma)$	$F_{\gamma\varphi}(-\gamma,-\varphi)$	$F_{\gamma\varphi}(-\varphi,-\gamma)$	A_1

$F_{\gamma\gamma}(\gamma,\varphi)$	$F_{\gamma\gamma}(\gamma,\varphi)$	$F_{\varphi\varphi}(\varphi,\gamma)$	$F_{\gamma\gamma}(-\gamma,-\varphi)$	$F_{\varphi\varphi}(-\varphi,-\gamma)$	A_1
$F_{\varphi\varphi}(\gamma,\varphi)$	$F_{\varphi\varphi}(\gamma,\varphi)$	$F_{\gamma\gamma}(\varphi,\gamma)$	$F_{\varphi\varphi}(-\gamma,-\varphi)$	$F_{\gamma\gamma}(-\varphi,-\gamma)$	
$p_X(\gamma,\varphi)$	$p_X(\gamma,\varphi)$	$-p_X(\varphi,\gamma)$	$p_X(-\gamma,-\varphi)$	$-p_X(-\varphi,-\gamma)$	B_1
$p_Y(\gamma,\varphi)$	$p_Y(\gamma,\varphi)$	$-p_Y(\varphi,\gamma)$	$-p_Y(-\gamma,-\varphi)$	$p_Y(-\varphi,-\gamma)$	B_2
$p_Z(\gamma,\varphi)$	$p_Z(\gamma,\varphi)$	$p_Z(\varphi,\gamma)$	$p_Z(-\gamma,-\varphi)$	$p_Z(-\varphi,-\gamma)$	A_1

3. CALCULATION DETAILS

The equilibrium configurations HT are presented in Fig.1 at the global (trans-conformer) and local (cis-conformer) energy minima as well as in the configuration being the initial one for performing the calculation of the 2D potential energy surface (PES). The hydroxyl groups rotate around the O-O bonds. Further, we will be denoting the equivalent torsional coordinates as γ and φ. The zero values γ and φ were chosen in the configuration presented on the right of Fig.1 where the hydroxyl atoms of hydrogen (H_1 and H_2) lie in the plane, which is formed by the O_3-O_5-O_4 atoms.

The potential energy satisfies the condition (see Table 2 and 3):

$$U(\gamma,\varphi)=U(-\gamma,-\varphi)=U(\varphi,\gamma)=U(-\varphi,-\gamma). \quad (3)$$

Taking this relationship into account, one can minimize all calculations by finding the energy values and optimized geometric parameters of the HT molecule in the triangle shown in Fig.2

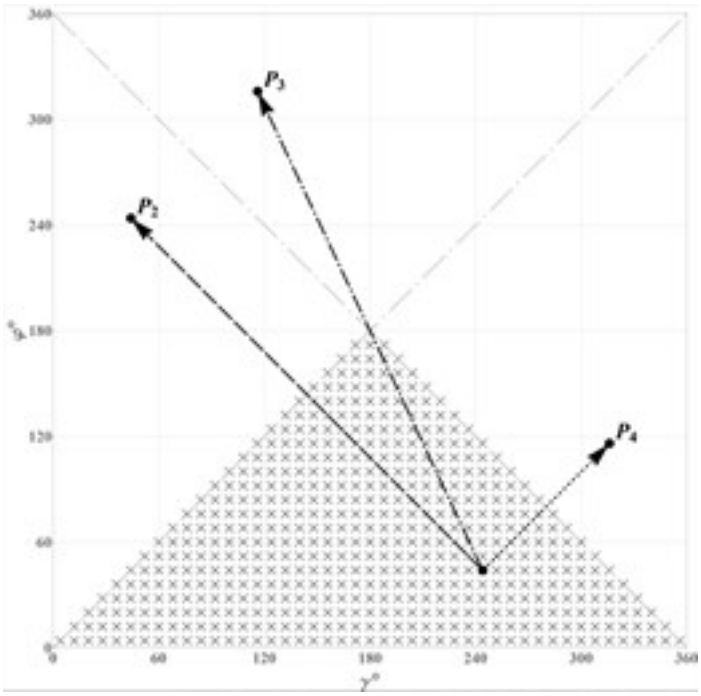

Figure 2. The minimal set of the points where potential energy and geometric parameters of the HT molecule have to be calculated. The equivalent points generated by symmetry operations P_2-P_4 (see Tables 1-3) are indicated by the arrows.

Using symmetry operation P_2 and then P_4 it is easy to obtain values of all molecular parameters in full square. Let's it will be the 1-st method of data preparation. For the reasons stated below sometimes we also calculated the data in the full square shown in Fig.2. In this

case, we used this data as they are (the 2-nd method, when symmetry conditions are not satisfied), or averaged them by four equivalent points (the 3-d method). Preparing the data by the 1-st method the torsional coordinates satisfied the conditions:

$$\begin{aligned} &0 \prec \gamma \prec 2\pi; \\ &0 \prec \varphi \le \gamma, \; if \;\; \gamma \le \pi; \\ &0 \prec \varphi \le 2\pi - \gamma, \; if \;\; \pi \prec \gamma \prec 2\pi; \end{aligned} \qquad (4)$$

Preparing the data by the 2 and 3 methods the torsional coordinates satisfied the conditions:

$$0 \prec \gamma \prec 2\pi, \qquad 0 \prec \varphi \prec 2\pi; \quad (5)$$

The values of the energy of the torsional states were calculated using the DVR and Fourier methods. For proper symmetry account relative to the O_2-O_3-O_4 plane, the values of the torsional coordinates on the K*K grid (K=45) were varied from 4° to 356° in the step of 8°. In all cases, we have got an equidistant 2D grid in the full square shown in Fig.2. The data obtained by 1-st and 3-d methods were used to obtain a denser equidistant 2D K*K grid (K=135) by interpolation using cubic splines in the frame of [44], where torsional coordinates were varied from $\frac{4}{3}^0$ to $358\frac{2}{3}^0$ instep $\frac{8}{3}^0$. Let's it will be the 4-th method of data preparation (when interpolation is used). To check interpolated values quality the less dense equidistant 2D K*K grid (K=15) was extracted from 2D 45*45 grid calculated data for symmetrized methods 1 and 3, where torsional coordinates were varied from 12^0 to 348^0 in step 24^0. This data was used to obtain again equidistant 2D K*K grid (K=45) by interpolation using the same method [44].

In the nodes of the equidistant 2D K*K grid (K=45), keeping fixed values of the torsional coordinates, HT geometry was optimized on all other coordinates using MP2 [45,46] and CCSD(T) [47,48] levels of theory and acc-pVTZ [49-51] basis sets in frame of quantum-chemical package [52]. Configurations optimized in each node were used to calculate the kinematic coefficients using Wilson vectors ($\vec{s}$ - vectors) [53]. The vibrational Schrödinger equation with reduced dimensionality for the torsional vibrations of two hydroxyl groups can be written as follows [43,54-56]:

$$\left[-F_{\gamma\gamma}(\gamma,\varphi)\frac{\partial^2}{\partial\gamma^2} - F_{\varphi\varphi}(\gamma,\varphi)\frac{\partial^2}{\partial\varphi^2} - F_{\gamma\varphi}(\gamma,\varphi)\frac{\partial^2}{\partial\gamma\partial\varphi} + U(\gamma,\varphi) \right] \Psi(\gamma,\varphi) = E\Psi(\gamma,\varphi); \quad (6)$$

The kinematic parameters can be determined from the following relations [43,54-56]:

$$F_{\gamma\gamma} = B_O\left[\left(\vec{s}_3^{\,\gamma}\right)^2 + \left(\vec{s}_5^{\,\gamma}\right)^2 + \left(\vec{s}_4^{\,\gamma}\right)^2 \right] + B_H\left(\vec{s}_1^{\,\gamma}\right)^2; \quad (7)$$

$$F_{\varphi\varphi} = B_O\left[\left(\vec{s}_4^{\,\varphi}\right)^2 + \left(\vec{s}_5^{\,\varphi}\right)^2 + \left(\vec{s}_3^{\,\varphi}\right)^2 \right] + B_H\left(\vec{s}_2^{\,\varphi}\right)^2; \quad (8)$$

$$F_{\gamma\varphi} = B_O\left[2\left(\vec{s}_3^{\,\gamma}\cdot\vec{s}_3^{\,\varphi}\right)+2\left(\vec{s}_5^{\,\gamma}\cdot\vec{s}_5^{\,\varphi}\right)+2\left(\vec{s}_4^{\,\gamma}\cdot\vec{s}_4^{\,\varphi}\right)\right];\ (9)$$

Here $\vec{s}_N^{\,x}$ is the Wilson vector for the coordinate $x=\{\gamma,\varphi\}$ and for the atom with the number N (the numeration of atoms corresponds to Fig.1 (on the right)), $B_X=\dfrac{\hbar^2}{2M_X l_0^2}$; $X\in\{H,O\}$, $\hbar$ is the Planck's constant, l_0 =1Å, M_H, M_O are the corresponding masses of hydrogen and oxygen atoms.

To solve the Schrödinger equation (6) by the DVR method [57-62] the Hamiltonian matrix was calculated by the formula:

$$H_{(i,j)(i',j')} = -F_{\gamma\gamma}(\gamma_i,\varphi_j)D^{\gamma\gamma}_{ii'}\delta_{jj'} - F_{\varphi\varphi}(\gamma_i,\varphi_j)\delta_{ii'}D^{\varphi\varphi}_{jj'} - F_{\gamma\varphi}(\gamma_i,\varphi_j)D^{\gamma}_{ii'}D^{\varphi}_{jj'} + U(\gamma_i,\varphi_j)\delta_{ii'}\delta_{jj'}\ (10)$$

Here:

$$D^{xy}=\tilde{D}^x D^y;\quad D^x_{ii'}=\frac{(-1)^{i'-i}}{2sin\left[\dfrac{\pi(i'-i)}{N_X}\right]};\ D^x_{ii}=0;$$
$$x\in(\gamma,\varphi);\quad i',i\in\{1\div N_X\};\ N_X=15\ or\ 45; \qquad (11)$$

To solve the Schrödinger equation (6) by the Fourier method [63-65] the Hamiltonian matrix was calculated by the formula [56]:

$$H_{(m,n)(m',n')} = -m^2F^{\gamma\gamma}_{m-m',n-n'} - n^2F^{\varphi\varphi}_{m-m',n-n'} - mnF^{\gamma\varphi}_{m-m',n-n'} + U_{m-m',n-n'}\quad (12)$$

where $F^{\gamma\gamma}_{m,n}, F^{\varphi\varphi}_{m,n}, F^{\gamma\varphi}_{m,n}, U_{m,n}$ coefficients were found by the fitting coefficients in the equation (6) by 2D complex Fourier series using [44]:

$$F_{\gamma\gamma}(\gamma,\varphi)=\sum_{m,n=-M}^{M}F^{\gamma\gamma}_{m,n}e^{i(m\gamma+n\varphi)},\qquad F_{\varphi\varphi}(\gamma,\varphi)=\sum_{m,n=-M}^{M}F^{\varphi\varphi}_{m,n}e^{i(m\gamma+n\varphi)},$$
$$F_{\gamma\varphi}(\gamma,\varphi)=\sum_{m,n=-M}^{M}F^{\gamma\varphi}_{m,n}e^{i(m\gamma+n\varphi)},\qquad U(\gamma,\varphi)=\sum_{m,n=-M}^{M}U_{m,n}e^{i(m\gamma+n\varphi)} \qquad (13)$$

The wave function is sought in the form:

$$\Psi(\gamma,\varphi)=\sum_{m,n=-N}^{N}\Psi_{m,n}e^{i(m\gamma+n\varphi)},\quad N\succ M; \qquad (14)$$

Since the Cartesian coordinate system varied its orientation in relation to the molecule as the hydroxyl groups rotate, components of dipole moment vector at each node of the 2D grid were recalculated for the Cartesian coordinate system related to the molecular skeleton, in which the Z-axis was directed along O_3-O_5-O_4 angle bisector, the X-axis lied in the plane of the O_3-O_5-O_4 atoms and the Y-axis supplemented the X and Y to the right-hand triple and was, therefore, normal to the plane of three heavy atoms.

Squares of matrix elements of the dipole moments operator were found using [44] and next formulae:

$$p_{if}^2 = \sum_{k=x,y,z} \left(\int_{\gamma=0}^{2\pi} \int_{\varphi=0}^{2\pi} \Psi_i(\gamma,\varphi)\, p_k(\gamma,\varphi) \Psi_f(\gamma,\varphi) d\gamma d\varphi \right)^2 \quad (15)$$

Here p_x, p_y, p_z are the dipole moment vector components in the molecular fixed Cartesian coordinate system, $\Psi_i(\gamma,\varphi)$, $\Psi_f(\gamma,\varphi)$ are the torsional wave functions in the initial (*i*) and final (*f*) states.

4. COMPARISON OF THE RESULTS OF CALCULATIONS OBTAINED DVR AND FOURIER METHODS

The calculated using DVR method values of the torsional stationary states energies for the data sets, obtained by 1-4 methods on the grids with different densities are represented in Table 4

Table 4 The calculated using DVR method at the B3LYP/acc-pVTZ and MP2/acc-pVTZ level of theory values of the stationary torsional states energies of the HT molecule.

		MP2/acc-pVTZ level of theory							B3LYP/acc-pVTZ level of theory	
Column and data set numbers		1	2	3	4	5	6	7	8	9
Method of the data preparation		3	4	1	3	2	4	4	2	3
Grid density parameter K		15	45	45	45	45	135	135	45	45
Interpolation based on data set		-	1	-	-	-	3	4	-	-
Data symmetry		C_{2v}	C_{2v}	C_{2v}	C_{2v}	C_1	C_{2v}	C_{2v}	C_1	C_{2v}
Energy level number	Configuration	Values of the stationary torsional states energies [cm^{-1}]								
1	trans	0	0	0	0	0	0	0	0	0
2	trans	$4.85*10^{-4}$	$7.75*10^{-11}$	$4.27*10^{-10}$	$1.10*10^{-10}$	$8.94*10^{-2}$	$2.31*10^{-9}$	$3.19*10^{-10}$	$1.08*10^{-1}$	$1.34*10^{-10}$
3	trans	339.181	361.290	361.997	362.021	362.038	361.993	362.018	373.591	373.618
4	trans	339.189	361.290	361.997	362.021	362.093	361.993	362.018	373.753	373.618
5	trans	370.333	390.848	391.225	391.208	391.187	391.222	391.205	401.761	401.780
6	trans	370.334	390.848	391.225	391.208	391.319	391.222	391.205	401.908	401.780
7	trans	702.836	715.013	715.895	715.922	715.940	715.890	715.917	738.723	738.731
8	trans	702.884	715.013	715.895	715.922	715.993	715.890	715.917	738.844	738.731
9	trans	774.837	721.126	721.561	721.575	721.583	721.556	721.570	743.971	743.992
10	trans	774.839	721.126	721.561	721.575	721.658	721.556	721.570	744.121	743.992
11	trans	783.894	771.068	771.979	771.935	771.892	771.972	771.929	772.103	772.286
12	trans	783.924	771.068	771.979	772.935	772.066	772.972	772.929	772.692	772.400
13	cis	815.413	821.089	821.172	821.172	821.184	821.173	821.175	793.800	793.824
14	cis	815.416	821.089	821.172	821.178	821.256	821.173	821.175	793.955	793.824
15	trans	946.526	1037.26	1038.23	1038.24	1038.25	1038.22	1038.23	1035.60	1035.72
16	trans	946.529	1037.26	1038.23	1038.24	1038.32	1038.22	1038.23	1035.95	1035.72
17	trans	948.479	1039.43	1040.40	1040.41	1040.43	1040.39	1040.41	1071.83	1071.79
18	trans	948.526	1039.43	1040.40	1040.41	1040.48	1040.39	1040.41	1071.86	1071.79
19	cis	1063.66	1058.03	1058.64	1058.64	1058.65	1058.63	1058.64	1074.04	1074.00
20	cis	1063.66	1058.03	1058.64	1058.64	1058.73	1058.63	1058.64	1074.07	1074.00
21	trans	1127.85	1095.18	1096.55	1096.55	1096.54	1096.54	1096.54	1130.78	1130.81
22	trans	1128.14	1095.18	1096.55	1096.55	1096.65	1096.54	1096.54	1130.94	1130.81
23	trans	1158.23	1135.13	1136.06	1136.00	1135.94	1136.06	1135.99	1169.91	1169.96
24	trans	1158.29	1135.13	1136.06	1136.00	1136.15	1136.06	1135.99	1170.12	1169.96
25	cis	1215.88	1216.89	1217.24	1217.23	1217.24	1217.24	1217.24	1182.88	1182.90
26	cis	1215.91	1216.89	1217.24	1217.24	1217.33	1217.24	1217.24	1183.08	1182.96
27	cis	1267.84	1293.42	1294.42	1294.43	1294.45	1294.41	1294.42	1293.64	1293.68
28	cis	1267.84	1293.42	1294.42	1294.44	1294.50	1294.41	1294.43	1293.87	1293.71
29	trans	1290.94	1319.91	1320.77	1320.78	1320.82	1320.76	1320.77	1364.62	1364.57
30	trans	1291.00	1320.29	1321.14	1321.15	1321.19	1321.13	1321.15	1364.96	1364.91

Before proceeding to the discussion of the data in Table 4 it is important to stress that due to energy optimization in every node of the grid the calculated values of the potential energies and kinematic coefficients in four symmetrical points, presented in Fig.2, are not equal to each other. This is due to the fact that the finish of the calculations occurs when the conditions that satisfy the convergence criteria are reached. Moreover, at different equivalent points, these

conditions can be achieved for several different configurations of molecules with slightly different energies and geometric parameters. In spite of these differences are very small they can affect the accuracy of some results of calculations. On another hand, it is clear that using method 3 one can get by averaging the data at four equivalent points more accurate values of the energy and kinematic parameters that in addition satisfy the symmetry conditions.

Turning to the analysis of the data given in Table 4 it should be noted that the 15*15 grid is too sparse to give accurate values of the torsional state energies. One can see the data in column 1 are very different from all other calculated values. The data in 2-7 columns of Tabl.4 looks quite similar. Comparing the data represented in a 2-nd column with the data represented in 3 and 4 columns it can be argued that transition to the more dense grid using interpolation allows getting much more accurate values of the torsional state energies. Based on this conclusion, we will assume that the most accurate data are presented in column 7. Comparing the data represented in 3 and 4 columns it can also be stated that the accuracy of the data obtained by the first and third methods is comparable. Separate consideration requires the question of the accuracy of calculating the tunneling frequencies, in particular in the ground state of the molecule. One can see that the tunneling frequency in the ground state is very sensitive to the calculation method and grid density. Excluding the results obtained on a 15*15 grid from consideration, it should be noted that the second method (columns 5 and 8) obviously fails in determining the value of this frequency. This means that an accurate account of symmetry is needed if we use the DVR method.

The calculated by Fourier method values of the torsional stationary states energies for the data set 4 (see the first row in Table 4) and for different M and N (see formulas (11) and (12)) are represented in Table 5.

Table 5 *The calculated at the MP2/acc-pVTZ level of theory values of the stationary torsional states energies for the data set 4 using the Fourier method for the different values of M and N.*

Data set		4									
Method of the data preparation		3									
Grid density parameter K		45									
Data symmetry		C_{2v}									
Column numbers		1	2	3	4	5	6	7	8	9	10
M (see (11))		7	10	13	18	22	22	27	27	28	28
N (see (12))		30	30	30	30	30	35	30	32	30	32
Energy level number	Configuration	Values of the stationary torsional states energies [cm^{-1}]									
1	trans	0	0	0	0	0	0	0	0	0	0
2	trans	$4.77*10^{-5}$	$4.19*10^{-5}$	$5.71*10^{-7}$	$8.91*10^{-7}$	$8.99*10^{-10}$	$9.01*10^{-10}$	$1.27*10^{-7}$	$1.26*10^{-7}$	$3.01*10^{-7}$	$1.26*10^{-7}$
3	trans	362.312	362.018	362.021	362.021	362.021	362.021	362.021	362.021	362.021	362.021
4	trans	362.312	362.018	362.021	362.021	362.021	362.021	362.021	362.021	362.021	362.021
5	trans	391.236	391.209	391.208	391.208	391.208	391.208	391.208	391.208	391.208	391.208
6	trans	391.236	391.209	391.208	391.208	391.208	391.208	391.208	391.208	391.208	391.208
7	trans	715.996	715.920	715.921	715.922	715.922	715.922	715.922	715.922	715.922	715.922
8	trans	715.996	715.920	715.921	715.922	715.922	715.922	715.922	715.922	715.922	715.922
9	trans	721.694	721.574	721.575	721.575	721.575	721.575	721.575	721.575	721.575	721.575
10	trans	721.694	721.574	721.575	721.575	721.575	721.575	721.575	721.575	721.575	721.575
11	trans	772.059	772.935	771.935	771.935	771.935	771.935	771.935	771.935	771.935	771.935
12	trans	772.059	772.935	771.935	771.935	771.935	771.935	771.935	771.935	771.935	771.935
13	cis	821.228	821.172	821.172	821.172	821.172	821.172	821.172	821.172	821.172	821.172
14	cis	821.228	821.178	821.178	821.178	821.178	821.178	821.178	821.178	821.178	821.178
15	trans	1038.30	1038.24	1038.24	1038.24	1038.24	1038.24	1038.24	1038.24	1038.24	1038.24

16	trans	1038.30	1038.24	1038.24	1038.24	1038.24	1038.24	1038.24	1038.24	1038.24	1038.24
17	trans	1040.45	1040.42	1040.41	1040.41	1040.41	1040.41	1040.41	1040.41	1040.41	1040.41
18	trans	1040.45	1040.42	1040.42	1040.41	1040.41	1040.41	1040.41	1040.41	1040.41	1040.41
19	cis	1058.76	1058.64	1058.64	1058.64	1058.64	1058.64	1058.64	1058.64	1058.64	1058.64
20	cis	1058.76	1058.64	1058.64	1058.64	1058.64	1058.64	1058.64	1058.64	1058.64	1058.64
21	trans	1096.51	1096.56	1096.55	1096.55	1096.55	1096.55	1096.55	1096.55	1096.55	1096.55
22	trans	1096.51	1096.56	1096.55	1096.55	1096.55	1096.55	1096.55	1096.55	1096.55	1096.55
23	trans	1136.15	1136.00	1136.00	1136.00	1136.00	1136.00	1136.00	1136.00	1136.00	1136.00
24	trans	1136.15	1136.00	1136.00	1136.00	1136.00	1136.00	1136.00	1136.00	1136.00	1136.00
25	cis	1217.28	1217.23	1217.23	1217.23	1217.23	1217.23	1217.23	1217.23	1217.23	1217.23
26	cis	1217.29	1217.24	1217.24	1217.24	1217.24	1217.24	1217.24	1217.24	1217.24	1217.24
27	cis	1294.51	1294.43	1294.43	1294.43	1294.43	1294.43	1294.43	1294.43	1294.43	1294.43
28	cis	1294.51	1294.44	1294.43	1294.44	1294.44	1294.44	1294.44	1294.44	1294.44	1294.44
29	trans	1320.90	1320.77	1320.78	1320.78	1320.78	1320.78	1320.78	1320.78	1320.78	1320.78
30	trans	1321.24	1321.15	1321.15	1321.15	1321.15	1321.15	1321.15	1321.15	1321.15	1321.15

As one can see from Table 5 all values but tunneling frequency in the ground (and exited) states are nearly insensitive to M and N. The differences in the values of the latter are five orders of magnitude. Comparing the data in Table 5 and data in the 4-th column of Table 4 becomes obvious that most similar to the results of calculation by the DVR method data represented in columns numbers 5 and 6. In this case $M \approx [K/2]$. Keeping in mind this relationship we have calculated energies of the torsional states and tunneling frequencies for the cases represented in Table 4. This data collected in Table 6.

Table 6 *The calculated at the MP2/acc-pVTZ level of theory values of the stationary torsional states energies for the data sets 1-7 using the Fourier method for the* $M \approx [K/2]$.

Data set		1	2	3	4	5	6	7
Method of the data preparation		3	4	1	3	2	4	4
Grid density parameter K		15	45	45	45	45	135	135
Interpolation based on data set		-	1	-	-	-	3	4
Data symmetry		C_{2v}	C_{2v}	C_{2v}	C_{2v}	C_1	C_{2v}	C_{2v}
M		7	22/ 23	22/ 23	22/ 23	22/ 23	22/ 33/ 37	22/ 33/ 37
N		30	30/ 30	30/ 30	30/ 30	30/ 30	33/ 38/ 40	33/ 38/ 50
Energy level number	Configuration	Values of the stationary torsional states energies [cm^{-1}]						
1	trans	0	0	0	0	0	0	0
2	trans	$7.69*10^{-11}$	$8.41*10^{-12}$ $2.13*10^{-10}$	$2.98*10^{-10}$/ $1.08*10^{-8}$	$8.99*10^{-10}$/ $9.01*10^{-10}$	$8.94*10^{-2}$/ $8.94*10^{-2}$	$2.54*10^{-10}$ $5.01*10^{-10}$ $1.58*10^{-10}$	$1.00*10^{-10}$ $3.98*10^{-10}$ $3.71*10^{-10}$
3	trans	362.344	361.290	361.997	362.021	362.038	361.993	362.018
4	trans	362.344	361.290	361.997	362.021	362.093	361.993	362.018
5	trans	391.516	390.848	391.225	391.208	391.187	391.222	391.205
6	trans	391.516	390.848	391.225	391.208	391.319	391.222	391.205
7	trans	716.055	715.013	715.895	715.922	715.940	715.890	715.917
8	trans	716.055	715.013	715.895	715.922	715.993	715.890	715.917
9	trans	721.815	721.126	721.561	721.575	721.583	721.556	721.570
10	trans	721.815	721.126	721.561	721.575	721.658	721.556	721.570
11	trans	772.444	771.068	771.979	771.935	771.892	771.972	771.929
12	trans	772.444	771.068	771.979	771.935	772.066	772.972	772.929
13	cis	821.405	821.089	821.172	821.172	821.184	821.173	821.175
14	cis	821.405	821.089	821.172	821.178	821.256	821.173	821.175
15	trans	1038.37	1037.26	1038.23	1038.24	1038.25	1038.22	1038.23
16	trans	1038.37	1037.26	1038.23	1038.24	1038.32	1038.22	1038.23
17	trans	1040.50	1039.43	1040.40	1040.41	1040.43	1040.39	1040.41
18	trans	1040.50	1039.43	1040.40	1040.41	1040.48	1040.39	1040.41
19	cis	1058.93	1058.03	1058.64	1058.64	1058.65	1058.63	1058.64
20	cis	1058.93	1058.03	1058.64	1058.64	1058.73	1058.63	1058.64
21	trans	1096.81	1095.18	1096.55	1096.55	1096.54	1096.54	1096.54
22	trans	1096.81	1095.18	1096.55	1096.55	1096.65	1096.54	1096.54
23	trans	1136.32	1135.13	1136.06	1136.00	1135.94	1136.06	1135.99
24	trans	1136.32	1135.13	1136.06	1136.00	1136.15	1136.06	1135.99
25	cis	1217.32	1216.89	1217.24	1217.23	1217.24	1217.24	1217.24
26	cis	1217.32	1216.89	1217.24	1217.24	1217.33	1217.24	1217.24
27	cis	1294.73	1293.42	1294.42	1294.43	1294.45	1294.41	1294.42
28	cis	1294.73	1293.42	1294.42	1294.44	1294.50	1294.41	1294.43
29	trans	1321.03	1319.91	1320.77	1320.78	1320.82	1320.76	1320.77
30	trans	1321.33	1320.29	1321.14	1321.15	1321.19	1321.13	1321.15

Comparing data in Table 4 and Table 6 it is possible to state that results of calculations of the tunneling frequency in the ground state using DVR and Fourier methods (in the last case $M \approx [K/2]$) become more similar. It should be emphasized that when we perform calculations on the 2D equidistant K * K grid (K = 135), the results of calculation of the tunneling frequency in the ground state using the Fourier method are weakly depend on M and N values. In addition, since results represented in columns 6 and 7 of Table 6 are very similar, we performed calculations of the energies and kinematic coefficients at CCSD(T)/acc-pVTZ level of theory only in triangle represented in Fig. 2 and then spread over the whole square using the 1-st method.

5. DISCUSSION OF THE RESULTS.

In Table 7 we collected data on the parameters of equilibrium trans- and cis-configurations of the HT molecule calculated at MP2/acc-pVTZ and CCSD(T)/acc-pVTZ levels of theory. In addition, based on literature data, we included in Table 7 the calculated geometrical parameters for the trans-conformer obtained at more advanced levels of theory.

Table 7 Calculated at MP2/acc-pVTZ and CCSD(T)/acc-pVTZ levels of theory equilibrium geometrical parameters of the trans- and cis-conformers of the HT molecule as well as some literature data on trans-conformer obtained at CCSD(T)/cc-pV5Z and CCSD(T)-F12/cc-pVTZ-F12 levels of theory.

Level of theory	Configuration	$l_{O_3-H_1}$, $l_{O_4-H_2}$	$l_{O_3-O_5}$, $l_{O_4-O_5}$	$\delta_{O_5O_4H_2}$, $\delta_{O_5O_3H_1}$	$\delta_{O_3O_5O_4}$	$\gamma_{H_1O_3O_5O_4}$	$\varphi_{H_2O_4O_5O_3}$	Taken from
MP2/acc-pVTZ	Trans	0.97050	1.42693	100.933	106.803	80.429	80.429	
CCSD(T)/acc-pVTZ		0.96989	1.43470	101.024	106.904	81.287	81.287	
MP2/acc-pVTZ	Cis	0.97004	1.42723	101.367	107.005	94.049	-94.049	
CCSD(T)/acc-pVTZ		0.96972	1.43524	101.431	107.135	94.151	-94.151	
CCSD(T)/cc-pV5Z	Trans	0.9665	1.4252	101.250	107.010	81.500	81.500	[36]
CCSD(T)-F12/ cc-pVTZ-F12	Trans	0.967	1.425	101.3	107.0	81.5	81.5	[29]

According to represented in Table 7 data the results of calculations of the equilibrium geometrical parameters of the HT molecule, obtained at different levels of theory, are very close to each other and the geometrical parameters in the trans- and cis-conformers differ significantly only in the values of the torsional coordinates.

The 2D PES of the HT molecule presented in Fig.3. It is symmetrical with respect to all the symmetry elements of the point group $C_{2V}(M)$ and, therefore, transformed according to the totally symmetrical representation A_1.

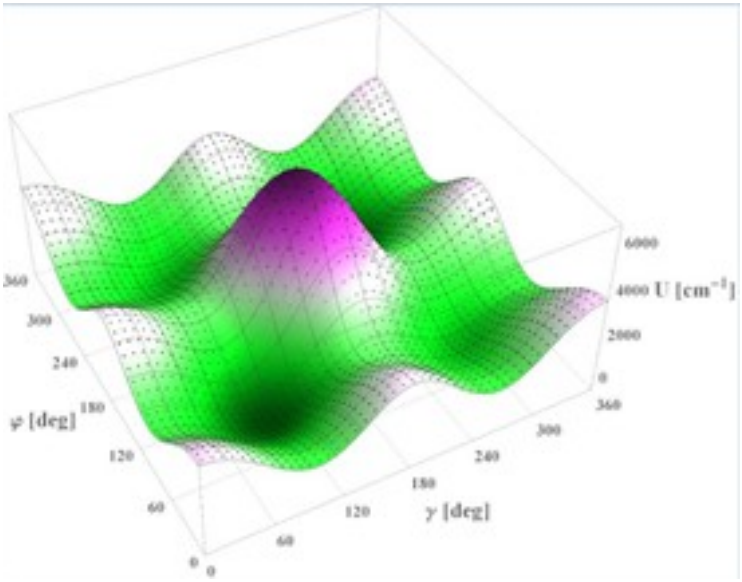

Fig.3. 2D PES of a HT molecule calculated at the CCSD(T)/acc-pVTZ level of theory. The 2D uniform grid nodes, at which the potential energy was computed, are shown by points in the 2D PES.

According to calculations at CCSD(T)/acc-pVTZ level of theory, the difference between minimums of the potential wells of the trans- and cis-conformers is equal to 830.3 cm^{-1}. The groud torsional levels of the trans- and cis- conformers lie 387.1 and 341.2 cm^{-1} above its potential wells minimums respectively. That means the energy difference between trance- and cis- conformers actually equals 784 cm^{-1}. To estimate barriers between potential wells we have found the minimum energy path from one well to another. This 1D way is represented in Fig. 4

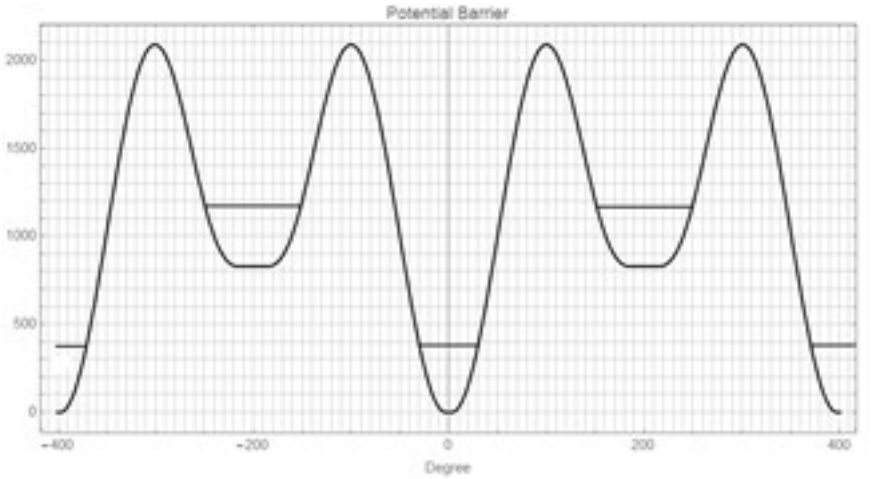

Figure 4 The minimum energy path from global well to local one and so on. The 1D coordinate α connected with the torsional coordinates as: $d\alpha = \sqrt{(d\gamma)^2 + (d\varphi)^2}$. The ground states levels of trans- and cis- conformers are shown.

The part of this 1D path on the 2D PES picture is represented in Fig. 5

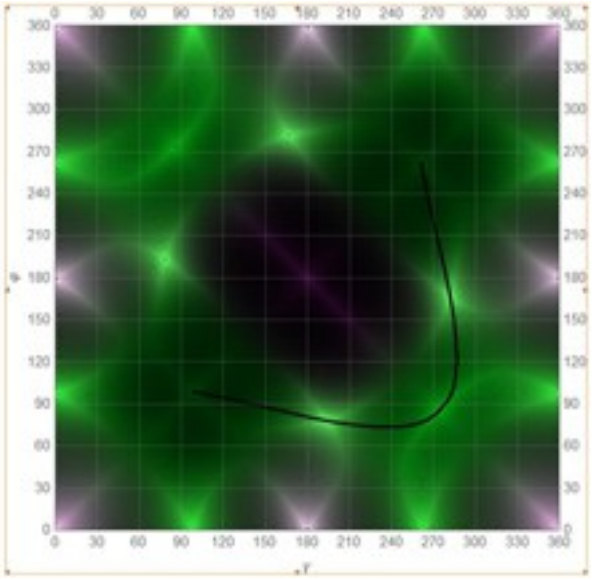

Figure 5 The minimum energy path on 2D PES from global well to the local one and so on.

From Fig. 4 and 5 one can see that the minimal potential barrier from trans- to cis- configuration is equal to 1703.8 cm^{-1} and from cis- to trans- conformer – 919.1 cm^{-1}. The last value of potential barrier indicates us the cis- conformer may be quite stable in the wide temperature interval.

The 2D surfaces of kinematic coefficients are presented in Fig. 6

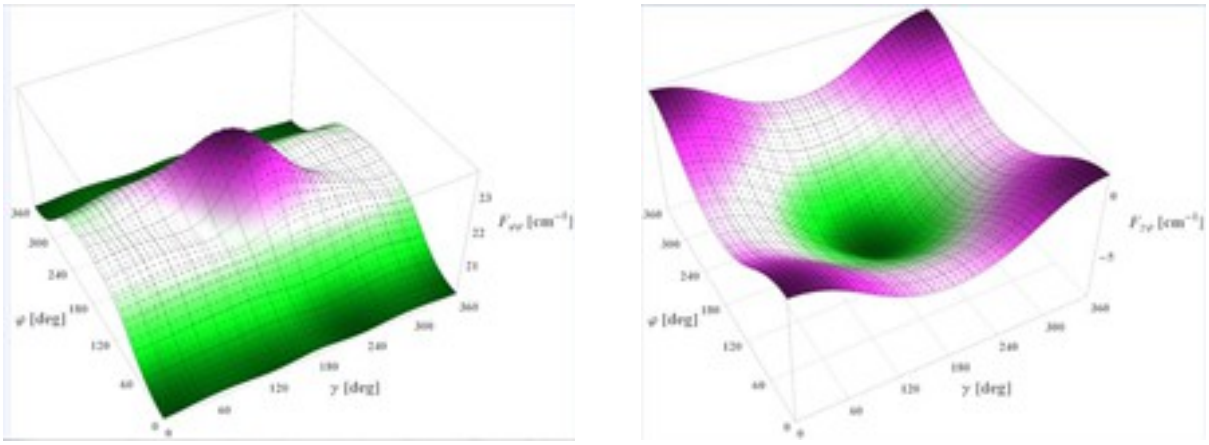

Figure 6 2D surfaces of the kinematic coefficients $F_{\varphi\varphi}$ and $F_{\gamma\gamma}$ (on the left), and $F_{\gamma\varphi}$ (on the right) calculated at the CCSD(T)/acc-pVTZ level of theory.

It should be noted that 2D surfaces of the kinematic coefficients $F_{\gamma\gamma}$ and $F_{\varphi\varphi}$ are equivalent. The 2D surfaces of the dipole moment components are presented in Fig. 7.

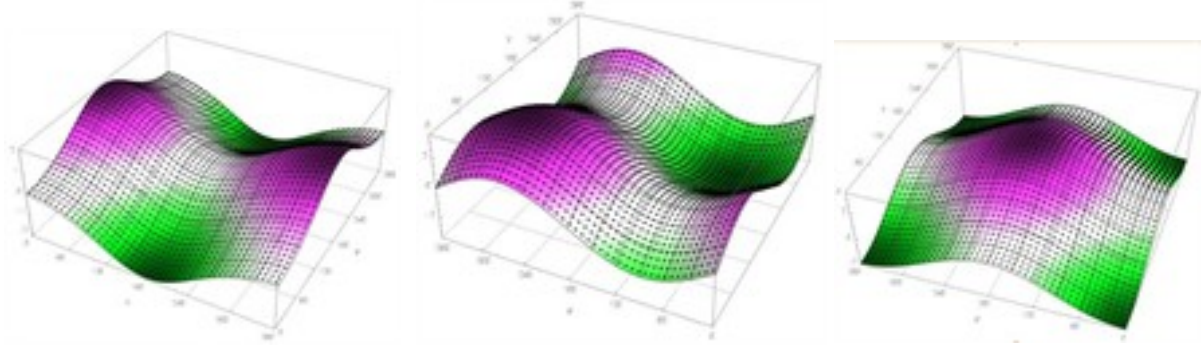

Figure 7 Calculated at CCSD(T) level of theory 2D surfaces of the X (left), Y (middle) and Z (right) components of the dipole momentum of the HT molecule.

The most accurate from our point of view values of energies of the stationary torsional states measured from the ground torsional state of the HT molecule are summarized in Table 8. As the results, represented in Tabl. 8, were obtained on the same 2D grid (135*135) and using the same method (4 method) the difference between energy values is due to the different levels of theory only (MP2/acc-pVTZ and CCSD(T)/acc-pVTZ). One can see the results of calculations for the trans-conformer are very close. However according to the CCSD(T) level of theory the positions of the cis-conformer torsional energy levels are significantly lower than according to the MP2 level of theory. Thus, all further consideration will be based on data obtained using the CCSD(T)/acc-pVTZ level of theory. Fig 8 is represented calculated at this level of theory wave functions for 3-6 torsional states (see the first column of Table 8).

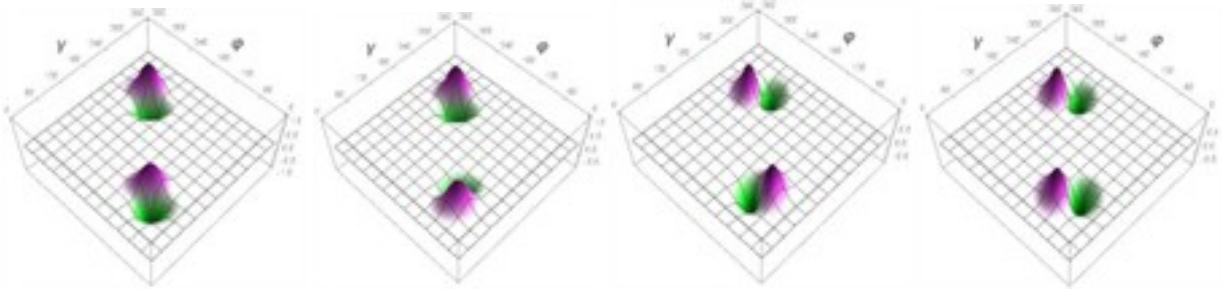

Figure 8 Calculated at CCSD(T) level of theory wave functions for symmetric (two left figures) and antisymmetric (two right figures) torsional vibrations in trans-conformer of the HT molecule. These states are numbered from left to right starting from three to six in accordance with the numbering of torsional states given in the first column of Table 8.

We were also able to determine torsional quantum numbers for several lowest torsional states. The n_{as} and n_s in columns 5 and 6 of Table 8 are antisymmetric and symmetric torsional quantum numbers in trans- and cis-conformers (see the Configuration column in Table 8). Symmetry species of the torsional states analyzed with the help of the data from Tables 1 and 2, are represented in columns 5 and 10. The tunneling splittings of the torsional levels are indicated in column 11 of Table 8. As expected the splitting of the torsional levels increases with the increasing their energy.

Table 8. Values of energies in [cm^{-1}] and symmetry of the stationary torsional states of HT molecule calculated at the MP2/acc-pVTZ and CCSD(T)/acc-pVTZ levels of theory

Column numbers		2	3	4	5	6	7	8	9	10	11
Data set		7	n_{as}	n_s	Symmetry species	Data set	9	n_{as}	n_s	Symmetry species	9
Method of the data preparation		4				Method of the data preparation	4				4
Interpolation based on data set		4				Interpolation based on data set	8				8
Grid density parameter K		135				Grid density parameter K	135				135
Level of theory		MP2/ acc-pVTZ				Level of theory	CCSD(T)/ acc-pVTZ				CCSD(T)/ acc-pVTZ
Data symmetry		C_{2v}				Data symmetry	C_{2v}				C_{2v}
Energy level number	Configuration	Energy [cm^{-1}]				Configuration	Energy [cm^{-1}]				Splitting of the torsional levels

1	trans	0	0	0	A_1+A_2	trans	0	0	0	A_1+A_2	$1.01*10^{-10}$
2	trans	$3.85*10^{-10}$	0	0	A_1-A_2	trans	$1.01*10^{-10}$	0	0	A_1-A_2	
3	trans	362.018	0	1	A_2	trans	361.538	0	1	A_2	$4.61*10^{-8}$
4	trans	362.018	0	1	A_1	trans	361.538	0	1	A_1	
5	trans	391.205	1	0	B_1	trans	391.293	1	0	B_1	$3.22*10^{-9}$
6	trans	391.205	1	0	B_2	trans	391.293	1	0	B_2	
7	trans	715.917	0	2	A_1	trans	715.686	0	2	A_1	$4.14*10^{-7}$
8	trans	715.917	0	2	A_2	trans	715.686	0	2	A_2	
9	trans	721.570	1	1	B_2	trans	721.956	1	1	B_2	$6.20*10^{-7}$
10	trans	721.570	1	1	B_1	trans	721.956	1	1	B_1	
11	trans	771.929	2	0	A_1	trans	772.374	2	0	A_1	$1.57*10^{-6}$
12	trans	772.929	2	0	A_2	trans	772.374	2	0	A_2	
13	cis	821.175	0	0	B_2	cis	784.659	0	0	B_2	$1.05*10^{-6}$
14	cis	821.175	0	0	A_1	cis	784.659	0	0	A_1	
15	trans	1038.23	1	2	B_1	cis	1030.86	1	0	B_1	$3.61*10^{-4}$
16	trans	1038.23	1	2	B_2	cis	1030.86	1	0	A_2	
17	trans	1040.41	0	3	A_2	trans	1040.11	1	2	B_2	$2.54*10^{-3}$
18	trans	1040.41	0	3	A_1	trans	1040.11	1	2	B_1	
19	cis	1058.64	1	0	B_1	trans	1042.27	2	1	A_1	$2.28*10^{-3}$
20	cis	1058.64	1	0	A_2	trans	1042.27	2	1	A_2	
21	trans	1096.54	2	1	A_1	trans	1096.86	0	3	A_1	$3.33*10^{-5}$
22	trans	1096.54	2	1	A_2	trans	1096.86	0	3	A_2	
23	trans	1135.99	3	0	B_2	trans	1137.55	3	0	B_2	$7.71*10^{-5}$
24	trans	1135.99	3	0	B_1	trans	1137.55	3	0	B_1	
25	cis	1217.24	0	1	A_1	cis	1185.36	0	1	A_1	$3.77*10^{-4}$
26	cis	1217.24	0	1	B_2	cis	1185.36	0	1	B_2	
27	cis	1294.42	2	0	A_1	cis	1273.56	2	0	A_1	$1.72*10^{-3}$
28	cis	1294.43	2	0	B_2	cis	1273.56	2	0	B_2	
29	trans	1320.77	2	2	A_2	trans	1326.07	2	2	A_2	$2.64*10^{-1}$
30	trans	1321.15	2	2	B_1	trans	1326.33	2	2	A_1	

To calculate the intensities of the torsional IR spectrum, it is also necessary to consider the symmetry of the torsional wave functions with respect to the permutation of the chemically equivalent atoms in the HT molecule. Since ^{16}O atoms have zero spins they can be excluded from further consideration. The total wave function must be symmetric or antisymmetric with respect to symmetry elements of the $C_{2V}(M)$ molecular symmetry group which does not include the inversion operation [40,66]. These are E and (12)(34) symmetry operations. Due to the last one interchanges an odd number of the fermion nuclei (protons) the total wave function must be antisymmetric with respect to this symmetry operation and consequently has to belong to B_1 or B_2 symmetry species. The torsional wave functions that belong to the A_1 and A_2 symmetry species are symmetric with respect to the interchange of fermion nuclei while the ones that belong to the B_1 and B_2 symmetry species are antisymmetric. The reducible representation of the hydrogen's nuclear spin functions can be decomposed into irreducible representations of the $C_{2V}(M)$ molecular symmetry group as follows:

$$\Gamma^{spin}_{C_{2V}(M)} = 3A_1 + 0A_2 + 1B_1 + 0B_2; \quad (16)$$

Thereby, the torsional wave functions must be combined with the spin wave functions as it is shown in Table 9.

Table 9 Possible combinations of the torsional and spin wave functions for the HT molecule.

Symmetry species of the torsional wave functions	A_1, A_2	B_1, B_2
Symmetry species of the spin wave functions	B_1	A_1
Symmetry species of the total wave functions	B_1, B_2	B_1, B_2
The degeneration of the torsional wave functions (g)	1	3
Specifier (s)	1	-1

As one can see from Table 9, the torsional wave functions that belong to A_1 and A_2 symmetry species are nondegenerate, while the torsional wave functions that belong to B_1 and B_2 symmetry

species are triple degenerate. In addition, the symmetry of the spin wave functions must be saved during the torsional transitions. Relative intensities of the IR bands for torsional transitions from the initial state i to the final state f were calculated using the next formulas [43,40,67-71]:

$$I_{i\to f} = \frac{Const \cdot \tilde{\nu}_{if} \cdot \frac{|s_i + s_f|}{2} \cdot g_i \cdot \left[e^{-\frac{E_i - E_1}{kT}} - e^{-\frac{E_f - E_1}{kT}} \right]}{Q(T)} p_{if}^2; \quad Q(T) = \sum_i g_i e^{-\frac{E_i - E_1}{kT}}; \tag{17}$$

where g_i is the multiplicity of degeneracy of the initial torsional state, the value of which is coordinated with the type of symmetry of the torsional wave function in accordance with the data of Table 8 and 9, s_i and s_f are the specifiers of the initial and final states, the value of which is 1 for the torsional states of the A_1 and A_2 type and -1 for the torsional states of the B_1 and B_2 as shown in Table 9, $Q(T)$ - partition function. With the use of these data, the relative intensities of the IR absorption bands at different temperatures were calculated from the formula (17). Fig. 9 presents the torsional IR spectrum of HT molecule at the temperatures of 300 and 30 K.

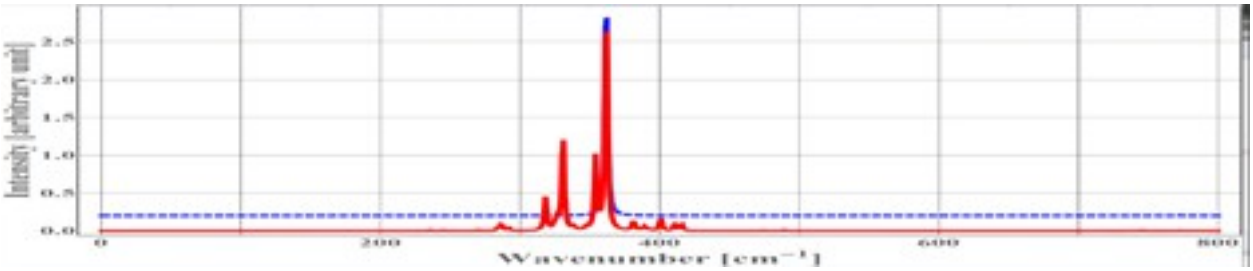

Figure 9. Torsional IR spectra of HT molecule at the temperatures of 300 K (red color) and 30 K (blue color) calculated at CCSD(T)/acc-pVTZ level of theory.

It is clear that the HT cis-conformer is less stable than the trans-conformer. However, the potential barrier for cis $\Rightarrow$ trans transition is higher than 800 cm^{-1} and the matrix insolation and low temperatures can stabilize cis-configuration. That is why the torsional spectrum of the cis-conformer of the HT molecule was also calculated at the temperature of 300 and 30 K. In this case, in the formula (17) when calculating the partition function, the summation was performed from i = 13 to i = 50 with the step of 1. It is presented in Fig. 10

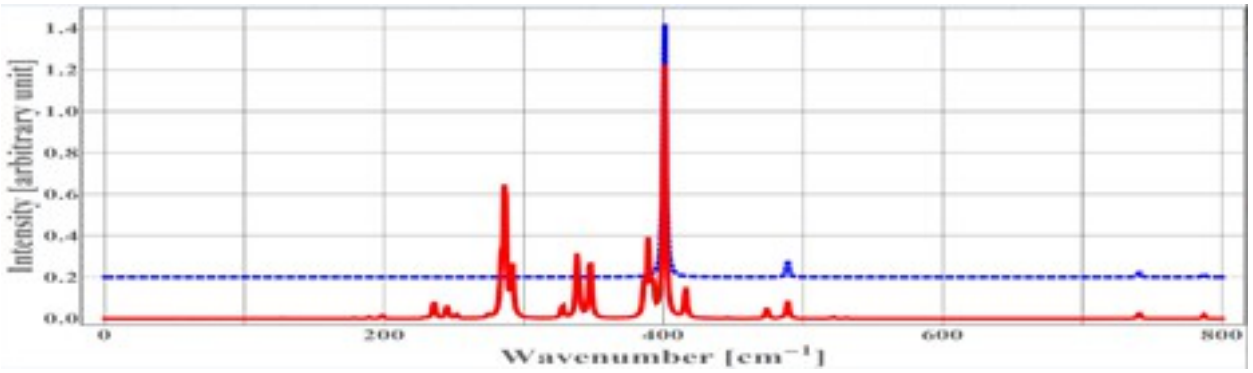

Figure 10. The torsional IR spectrum of the cis-transformer of HT molecule at the temperatures of 300 K (red color) and 30 K (blue color)at CCSD(T)/acc-pVTZ level of theory.

In addition as one can see from Table 8, the fifth torsional state is metastable due to all four lower torsional states have different symmetry of the spin functions. With this, the torsional spectrum of the trans- conformer of HT was calculated for which the 5th torsional level is ground at a temperature of 300 and 30 K. In this case, in the formula (17) when calculating the partition function, the summation was performed from i = 5 to i = 50 with the step of 1. It is presented in Fig. 11.

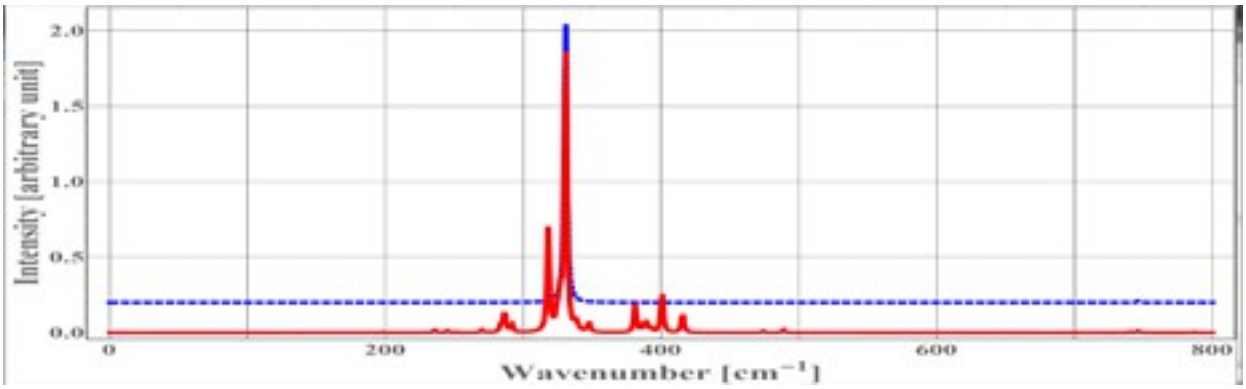

Figure 11. Torsional IR spectra of HT molecule at the exited 5th torsional state at the temperatures of 300 K (red color) and 30 K (blue color) calculated at CCSD(T)/acc-pVTZ level of theory.

As seen from Figs 9, 10 and 11 the calculated torsional spectrum of the HT molecule at the temperature of 30 K is featured by a small number of the absorption bands even if we assume the presence of both conformers of the molecule in the sample. The only intensive absorption band in the ground state of the trans-conformer at the temperature of 30 K corresponds to the symmetrical torsional vibration with the calculated frequency of 361.5 cm^{-1}. In the calculated torsional IR spectrum of the HT cis-conformer, there are four absorption bands. The most intensive band (400.7 cm^{-1}) corresponds to the excitation of the symmetrical torsional vibration. The medium-intensity band (488.9 cm^{-1}) corresponds to the excitation of the first overtone of the antisymmetric torsional vibration in the HT cis-conformer. The two low-intensity bands (740.5 and 786.8 cm^{-1}) correspond to excitation of the first overtone of the symmetrical torsional vibration and composite torsional vibration of the cis- and trans-conformers of the HT molecule. In the calculated torsional spectrum of the trans-conformer which is stuck in the fifth excited torsional state at 30 K, there are only two absorption bands. The intensive IR band has a maximum near 330.7 cm^{-1} while weak one has a maximum near 746.6 cm^{-1}.

Let us compare calculated and experimental (in matrix isolation [20]) IR spectra of the HT molecule. It is obvious that the calculated values of frequencies of the most intense absorption bands in the torsional IR spectrum of the HT at low temperatures turn out to be below

500 cm^{-1}. Unfortunately, the paper [20] presents the torsional spectrum of the HT molecule in the matrix isolation within the interval 740-800 cm^{-1} only. According to [20] 346.4 and 387.0 cm^{-1} IR bands were assigned to symmetric and antisymmetric torsional vibrations of the hydroxyl groups, while 776.1 cm^{-1} band was assigned to antisymmetric stretching O-O vibration. In addition, in the IR spectrum of the HT molecule represented in [20], one can see the broad band with a maximum near 752 cm^{-1} which was not assigned by authors. According to the above, in the torsional IR spectrum of the ground state trans-conformer at 30 K, there are no absorption bands in the spectral region higher 400 cm^{-1}. Thus the 752 cm^{-1} IR band can indicate the presence in sample cis- conformer or trans- conformer in fifth excited torsional state and may be assigned to the one of three mentioned above (740.5, 746.6 and 786.8 cm^{-1}) torsional vibrations in these conformers. Furthermore, since in the first four torsional states the HT molecule has to be the para-spin isomer while in fifth and six torsional states the HT molecule has to be the ortho-spin isomer the excitation of the antisymmetric torsional vibration from the two lowest states is forbidden. That means that assignments of the 387.0 cm^{-1} band to the antisymmetric torsional vibration is questionable. According to our calculations, this band may be assigned to the symmetric torsional vibration (400.7 cm^{-1}) in the cis-conformer, however, it is obvious that additional investigation is required.

6. CONCLUSIONS

The calculation of the torsional IR spectrum of the HT molecule has been performed at several levels of theory. It is quite expected that the calculated energy of the torsion levels depends on the level of theory used. However, as can be seen from Table 7(8), when calculating at various levels of the theory, the relative location of different torsion energy levels also changes. Performing calculations in frame of the DVR method, it is important correctly to choose the position of points of a 2D equidistant grid, taking into account the symmetry of the potential energy surfaces and kinematic coefficients. Accounting for the $C_{2V}(M)$ symmetry of the HT molecule made it possible to propose a minimum set of points on a 2D equidistant grid in which the molecular parameters should be calculated (see Fig. 2). An important parameter in calculations using the DVR method is the density of 2D grid points. In particular, it is shown that the use of 2D 15*15 mesh leads to unsatisfactory results (see column 1 in Table 4). At the same time, the Fourier method allows even in this case to obtain reasonable values of the energies of the torsion states (see column 1 in Table 5). Improving the accuracy of calculating the energy values of torsion states can be achieved by calculating the molecular parameters on a denser 2D equidistant grid (45 * 45 and 135 * 135). At the same time, as shown in the work, the correct use of interpolation methods that take into account the periodicity of molecular parameters and their

symmetry properties makes it possible to increase the accuracy of calculations of the energy values of torsion levels without increasing computational costs.

As one can see the splitting due to tunneling of the torsional levels, especially in the case of the ground state, is very sensitive to the quality of prepared data on 2D PES and 2D surfaces of the kinematic parameters. They have to satisfy the symmetry conditions and in addition, must be as smooth as possible. It should be noted that during data symmetrization and during the solving the Schrödinger equation using the Fourier method all 2D surfaces are smoothed. Due to the last circumstance, under equal conditions, the Fourier method shows better results in comparison with the DVR method.

The classification of the torsional and spin states of the HT molecule by the irreducible representation of the $C_{2V}(M)$ molecular symmetry group has been performed. The torsional IR spectra of the HT molecule at the temperatures of 300 and 30 K have been calculated. The preliminary comparative analysis of the calculated and experimental IR spectra of the HT at the temperature of 30 K has been performed. This analysis allows us to assume that the argon matrix stabilizes the cis-conformer of the molecule and the latter can be presented in the sample.

Based on the results of the calculations presented in Section 4, the calculated values of the tunneling frequencies should be treated with caution if their values are in the order of 10^{-9} – 10^{-10} cm^{-1}. It is obvious that the accuracy of calculations of the tunneling frequencies is directly related to the accuracy of calculations of the energy values of torsion states. In this case, it is also important to take into account the accuracy of calculations of energy and geometrical parameters at the nodes of uniform 2D grids using quantum chemical packages. In particular, tightening the convergence criteria when optimizing the geometry of a molecule should lead to an increase in the accuracy of calculations of the values of the tunneling frequencies. The results of this paper show that taking into account molecular symmetry in determining the values of molecular parameters is important in improving the accuracy of calculating the tunneling frequencies. The calculation of molecular parameters on the full 2D grid followed by averaging the values over four equivalent points on the 2D coordinate plane (see Fig. 2) should also lead to an increase in the accuracy of tunneling frequency calculations. Achieving agreement on the calculated values of the tunneling frequencies obtained using DVR and Fourier methods can serve as a good criterion for the reliability of the results obtained.

Based on the data presented in Table 4, and based on the analysis of the results of Section 4, it can be assumed that the tunneling frequency in the ground state is in the range of 10^{-10} – 10^{-9} cm^{-1} or 3-30 Hz. According to the data of calculations at the CCSD (T) / acc-pVTZ level of the theory, the tunneling frequency in the cis-conformer is several orders of magnitude greater than in the trans-conformer and turns out to be $1.047 * 10^{-6}$ cm^{-1} or 31388 Hz. Finally, the frequency

of tunneling in the metastable excited antisymmetric torsion vibrational state of the trans-conformer (see Table 8) is comparable in magnitude with the frequency of tunneling in the ground state and presumably must fall in the frequency range 5.5 - 55 Hz. All tunneling frequencies as well as few allowed for trans- and cis- conformers torsional vibrations may serve as a reference value when searching the HT in the cosmic space and in comets where the cis-conformer can theoretically exist at low temperatures too.

References

[1] M. Martins-Costa, J.M. Anlada, M.F. Ruiz-López, Int.J.Quant.Chem., 111 (2011) 1543-1554

[2] A.V. Levanov, D.V. Sakharov, A.V. Dashkova, E.E. Antipenko, V.V. Lunin, Eur.J.Inorg.Chem., 2011 (2011) 5144-5150

[3] D. Cannon, T. Tuttle, J. Koller, B. Plesničar, Comp.Theor.Chem., 1010 (2013) 19-24.

[4] D.J. Mckay, J.S. Wright, JACS, 120 (1998) 1003-1013.

[5] C. Murray, E.L. Derro, T.D. Sechler, M.I. Lester, Acc.Chem.Res., 42 (2009) 419-427.

[6] W. Zheng, D. Jewitt, R.I. Kaiser, Phys.Chem.Chem.Phys., 9 (2007) 2556-2563.

[7] P. Wentworth Jr., L.H. Jones, A.D. Wentworth, X. Zhu, N.A. Larsen, I.A. Wilson, X. Xu, W.A. Goddard III, K.D. Janda, A. Eschenmoser, R.A. Lerner, Science 293 (2001) 1806-1811.

[8] X. Zhu, P. Wentworth Jr., A.D. Wentworth, A. Eschenmoser, N.A. Larsen, I.A. Wilson, Proc.Natl.Acad.Sci. USA 101 (2004) 2247-2252.

[9] W.B. DeMore, J.Phys.Chem., 86 (1982) 121-126.

[10] C.F. Jackels, D.H. Phillips, J.Chem.Phys., 84 (1986) 5013-5024.

[11] D.W. Toohey, J.G. Anderson, J.Phys.Chem., 93 (1989) 1049-1058

[12] C. Gonzalez, J. Theisen, L. Zhu, H.B. Schlegel, W.L. Hase, J.Phys.Chem., 95 (1991) 6784 – 6792.

[13] X. Xu, R.P. Muller, W.A. Goddard III, PNAS 99 (2002) 3376-3381.

[14] T. Fujii, M. Yashiro, H. Tokiwa, JACS 119 (1997) 12280-12284.

[15] J.M. Anglada, S. Olivella, A. Solė, J.Phys.Chem. A, 111 (2007) 1695-1704.

[16] B. J. McCall, Phil., Trans. R. Soc. A 364 (2006) 2953.

[17] P.A. Giguère, K. Herman, Can.J.Chem., 48 (1970) 3473-3482.

[18] X. Deglise, P.A. Giguère, Can.J.Chem., 49 (1971) 2242-2247.

[19] J.L. Arnau, P.A. Giguère, J.Chem.Phys., 60 (1974) 270-273.

[20] A. Engdahl, B. Nelander, Science 295 (2002) 482-483.

[21] K. Suma, Y. Sumiyoshi, Y. Endo, JACS 127 (2005) 14998-14999.

[22] L. Radom, W.J. Hehre, J.A. Pople, JACS 93 (1971) 289

[23] R.J. Blint, M.D. Newton, J.Chem.Phys., 59 (1973) 6220

[24] B. Plesničar, S.Kaiser, A. Ažman, JACS 95 (1973) 5476

[25] D. Cremer, J.Chem.Phys., 69 (1978) 4456-4471

[26] D. Cremer, J.Chem.Phys., 69 (1978) 4440-4455

[27] M.A. Vincent, I.H. Hillier, J.Phys.Chem., 99 (1995) 3109-3113.

[28] S.L. Khursan, V.V. Shereshovets, Russ.Chem.Bull., 45 (1996) 1286-1291.

[29] D.S. Hollman, H.F. Schaefer III, J.Chem.Phys., 136 (2012) 084302.

[30]] B. Plesničar, T. Tuttle , J. Cerkovnik, J. Koller, D. Cremer, JACS 125 (2003) 11553-11564.

[31] T.H. Lay, J.W Bozzelli, J.Phys.Chem., 101 (1997) 9505-9510.

[32] A.V. Levanov, O.Y. Isaikina, V.V. Lunin, Russ.J.Phys.Chem. A, 90 (2016) 2136-2141.

[33] P.T. Nyffeler, N.A. Boyle, L. Eltepu, C.-H. Wong, A. Eschenmoser, R.A. Lerner, P. Wentworth Jr., Angew.Chem.Int., 43 (2004) 4656-4659.

[34] G. Strle, J. Cerkovnik, Angew.Chem., 127 (2015) 10055-10058.

[35] C.F. Jackels, J.Chem.Phys., 99 (1993) 5768-5779.

[36] P.A. Denis, F.R. Ornellas, J.Phys.Chem. A, 113 (2009) 499-506.

[37] B. Plesničar, Acta Chim.Slov., 52 (2005) 1-12.

[38] J. Cerkovnik, B. Plesničar, Chem.Rev., 113 (2013) 7930-7951.

[39] H.C. Louguet-Higgins, Mol.Phys., 6 (1963) 445

[40] P.R. Bunker, P. Jensen. Molecular Symmetry and Spectroscopy. NRC Research Press, 1998

[41] J.T. Hougen, J.Chem.Phys., 37 (1962) 1433

[42] R.G. Bone, T.W. Rowlands, N.C. Handy, A.J. Stone, Mol.Phys., 72 (1991) 33-73.

[43] G.A. Pitsevich, A.E. Malevich, V.V. Sapeshko, J.Mol.Spectr., 360 (2019) 31-38.

[44] Mathematica, Wolfram Research, Inc., http://www.wolfram.com/mathematica

[45] G. Hetzer, P. Pulay, H.J. Werner, Chem.Phys.Lett., 290 (1998) 143-149.

[46] M. Schutz, G. Hetzer, H.J. Werner., J.Chem.Phys., 111 (1999) 5691-5705.

[47] K. Raghavachari, G.W. Trucks, J.A. Pople, M. Head-Gordon, Chem.Phys.Lett., 157 (1989) 479.

[48] G.E. Scuseria, J.Chem.Phys., 94 (1991) 442-447.

[49] R.A. Kendall, T.H. Dunning, R.J. Harrison, J.Chem.Phys., 96 (1992) 6796-6806.

[50] D.E. Woon, T.H. Dunning Jr., J.Chem.Phys., 98 (1993) 1358-1371.

[51] T.H. Dunning Jr., J.Chem.Phys., 90 (1989) 1007.

[52] http://www.msg.ameslab.gov/GAMESS/GAMESS.html

[53] E.B. Wilson, J.J.C. Decius, P.C. Cross, Molecular Vibration Dover Publications, Inc., New York, 1955.

[54] T.J. Lukka, J.Chem.Phys., 102 (1995) 3945-3955.

[55] J. Makarewicz, A. Skalozub, Chem.Phys.Lett., 306 (1999) 352-356.
[56] G.A. Pitsevich, A.E. Malevich, J.Appl.Spectr., 82 (2015) 540-553.
[57] D.O. Harris, G.G. Enderholm, W.D. Gwinn, J. Chem. Phys. 43 (1965) 1515-1517.
[58] A.S. Dickinson, P.R. Certain, J. Chem. Phys. 49 (1968) 4209.
[59] R. Meyer, J. Chem. Phys. 52 (1970) 2053-2059.
[60] J.C. Light, I.P. Hamiltonian, J.V. Lill, J. Chem. Phys. 82 (1985) 1400
[61] D.T. Colbert, William H. Miller, J. Chem. Phys. 96 (1992) 1982-1991
[62] G.A. Pitsevich, A.E. Malevich, J.Appl.Spectr., 82 (2016) 893-900.
[63] C. Lanczos, Discourse on Fourier Series, Oliver and Boyd Ltd, Edinburgh and London, 1966
[64] G.A. Pitsevich, A.E. Malevich, Optics and Photonic Journal, 2 (2012) 332-337.
[65] G. Pitsevich, V. Balevicius, J.Mol.Struct., 1072 (2014) 38-44.
[66] Carlo Di Lauro, Rotational Structure in Molecular Infrared Spectra, Elsevier, 2013.
[67] J.M. Flaud, C. Camy-Peyret, J.Mol.Spectr., 55 (1975) 278.
[68] G. A. Pitsevich, I.Yu. Doroshenko, A. E. Malevich, E.Z. Shalamberidze, V.V. Sapeshko, V. E. Pogorelov, L.G.M. Pettersson, Spectrochim. Acta, Part A, 172 (2017) 83−90.
[69] W. Gordy,R.L. Cook, Microwave Molecular Spectra. Interscience Publishers, 1970
[70] G. A. Pitsevich, E.Z. Shalamberidze, A. E. Malevich, V. Sablinskas, V. Balevicius, L.G.M. Pettersson, Mol.Phys., 115 (2017) 2605-2613.
[71] G. Duxbury, Infrared Vibration-Rotation Spectroscopy, John Wiley & Sons, LTD, 2000.